Chapter 7
An Introduction to Accretion Disks

E. Alecian

Abstract In this chapter I first present the pre-main sequence stars around which accretion disks are observed and summarise the main observed characteristics of the classical T Tauri and Herbig Ae/Be stars. I then review the theoretical and empirical reasons that lead many scientists to conclude that the objects of this class are surrounded by accretion disk. Finally I review the basic characteristics of the disks of these stars, and expose the observations that lead us to derive them.

7.1 Introduction

7.1.1 The Star Formation

It is now well accepted among the scientific community that stars form inside initially stable molecular clouds. An external trigger breaks the stability of the cloud that collapses under gravity forces. The contraction of the matter gives birth to a class 0 object: a proto-star strongly accreting matter from a massive envelope (with a mass larger than the mass of the proto-star). The matter from the envelope is accreted onto the growing proto-star and also onto a disk to subsequently form a class I object constituted of a proto-star accreting matter mainly from a disk, the whole surrounded by an envelope much less massive than the stellar mass. Little by little the envelope is dissipating through jets, winds or accretion, and a star surrounded by an accretion disk forms a class II object. The accretion disk will also dissipate by accretion onto the star, coagulation onto proto-planets, photoevaporation, or other clearing mechanisms to finally give a class III object constituted by a star with a debris disk. At this stage the accretion stops.

During the proto-stellar (class 0 and I) phase, the central objects are highly obscured, and the systems radiate essentially from the submillimetric to the mid-infrared. This phase lasts about 10^5–10^6 years. At these stages, we believe that there

E. Alecian (✉)
LESIA-Observatoire de Paris, CNRS, UPMC Univ., Paris-Diderot Univ., 5 place Jules Janssen, 92195 Meudon Principal Cedex, France
e-mail: evelyne.alecian@obspm.fr

J.-P. Rozelot, C. Neiner (eds.), *The Environments of the Sun and the Stars*, Lecture Notes in Physics 857,
DOI 10.1007/978-3-642-30648-8_7,

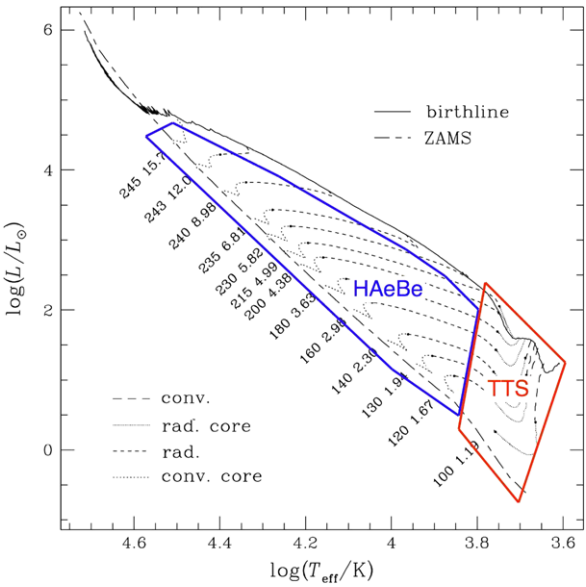

Fig. 7.1 PMS theoretical evolutionary tracks computed by Behrend and Maeder [13] and plotted in an Hertzsprung–Russell (HR) diagram. The tracks start on the birthline and end on the Zero-Age Main-Sequence (ZAMS). The transport of energy inside the star (radiative or convective or both) is indicated with *different broken lines*. The zones surrounded with *blue* (*brown*) *lines* represent the region where the Herbig Ae/Be (T Tauri) stars are situated (adapted from [13])

is no strong difference between low- and high-mass stars, as even at high-mass it is very likely that stars are forming from a low-mass proto-star that will accrete much more matter than future low-mass stars (e.g., [13]). Once the major accreting phase is done and the central star radiates mainly in the visible bands, the star starts its pre-main sequence phase (class II and III).

7.1.2 The Pre-Main Sequence Phase of Stellar Evolution

At this stage, it is very convenient to follow the evolution of the star inside the Hertzsprung–Russell (HR) diagram, i.e. a plot of the stellar luminosity in function of its effective temperature (Fig. 7.1). A star that comes just out from the proto-stellar phase is situated on the birthline, then follows a pre-main sequence (pre-MS) evolutionary tracks corresponding to its mass, and finally reaches the zero-age main-sequence (ZAMS), starting the longest phase of the evolution of a star, the main-sequence (MS). The time that a star spends on the pre-MS is highly dependent of its mass and varies from $\sim$100 Myr (at 1 $M_{\odot}$) to $\sim$0.15 Myr (at 15 $M_{\odot}$).

During the pre-MS, a star radiates mainly energy from its gravitational contraction. The nuclear reaction that will transform hydrogen into helium in the core of the star will only start at the end of the pre-MS phase. Above 20 $M_{\odot}$, a star on the birthline has already started to burn hydrogen in its core and therefore does not undergo a pre-MS phase.

The transfer of energy inside a pre-MS star changes with time and is highly dependent of the mass of the star. At low-mass, up to $\sim$1.4 $M_{\odot}$, the star first descends

the Hayashi track in the HR diagram with a fully convective interior. Then a radiative zone develops in the core and grows progressively until the star reaches the ZAMS. Above 1.2 $M_{\odot}$, the radiative core grows even bigger, to form a totally radiative star. Later, a convective core forms once the nuclear reaction are triggered. Above 1.4 $M_{\odot}$, the star does not go through the Hayashi phase, while above 4 $M_{\odot}$, the star starts its pre-MS already totally radiative.

The presence of a convective zone under the surface of the star plays an important role on its activity along the pre-MS (and also later on the MS) and hence on its interaction with its environment. A convective envelope can engender magnetic fields through dynamo processes. These magnetic fields can only exist at low mass and allow the exchange of matter of the star with its environment through magnetospheric accretion and winds. At higher mass, exchange occurs mainly through winds and only occasionally through accretion. This exchange of matter occurs in regions very close to the star (within few astronomical units (AU)).

Among the class II and III objects, we distinguish the T Tauri stars from the Herbig Ae/Be stars. The T Tauri stars have cool photospheres (∼3000–6000 K) that present specific observed properties revealing their young age such as IR-excess, spectral lines in emission, irregular light-variation, and an association with a bright or dark nebulosity [52]. The Herbig Ae/Be stars have similar properties and are considered the analogues of the T Tauri stars at higher temperature (above 6000 K, see [46, 77]). The approximate situation of both classes of objects in the HR diagram is schematically represented in Fig. 7.1. One of the major differences between Herbig Ae/Be stars and T Tauri stars is the magnetic activity. The T Tauri stars have masses below 1.5 Msun, and almost all of them have a convective envelope and therefore can create a magnetic field dynamo. All Herbig Ae/Be stars are mainly radiative and cannot create such magnetic fields. This results in that the activity close to the stellar surfaces is different in both kind of stars. Note however that fossil magnetic fields have been discovered in a small portion of Herbig Ae/Be stars (e.g. [4, 5]). The role of these fields in the stellar activity is not clear at the moment.

In the following we will concentrate on the environment situated at about 1 AU and above, where the circumstellar matter is concentrated into disks that surround the class II objects and the transition objects from class II to class III.

7.1.3 The Class II Objects

In this section I will describe the main properties of the T Tauri and Herbig Ae/Be stars in order to give the reader a global view of the behaviour of these objects that helped the scientists to propose models for the environment of these young stars.

Among the T Tauri stars, we distinguish two sub-classes: the classical T Tauri (CTTS|see classical T Tauri stars) stars, showing strong Hα emission, and the weak-line T Tauri stars (WTTS) with only faint spectral emission. Typical optical spectra of CTTS and WTTS are shown in Fig. 7.2. The classical T Tauri stars show very strong emission in the Balmer lines Hα and Hβ and also in may metallic lines, contrary to the WTTS. The Balmer jump on the blue part of the spectrum is in emission

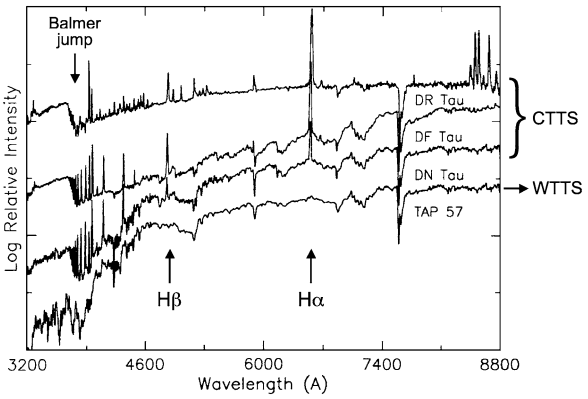

Fig. 7.2 Optical spectrum of CTTS and WTTS. Note the differences between CTTS and WTTS spectra in the Balmer lines Hα and Hβ, in the Balmer jump and in the continuum that is veiled for the CTTS (adapted from [14])

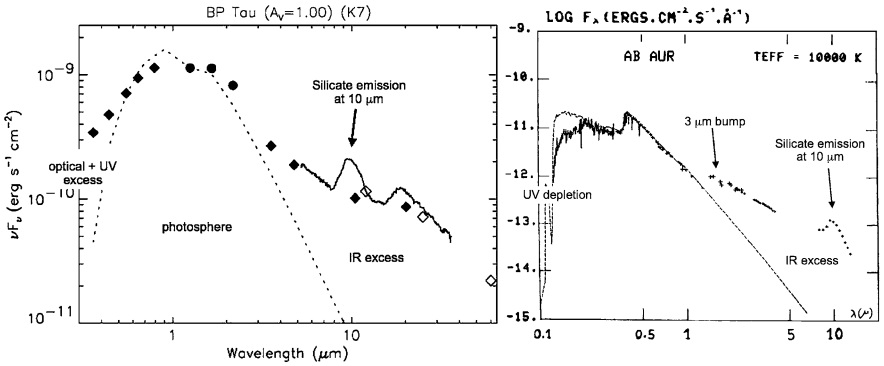

Fig. 7.3 Typical SEDs of CTT (*left*) and HAeBe (*right*) stars. The *crosses*, *diamonds* and *full lines* represent the observations. The theoretical spectrum of the photosphere of the star computed with the stellar temperature are overplotted with *dashed lines*. The observations illustrate the typical IR excess and deviations from a purely photospheric spectrum in the UV. Typical features are also indicated with arrows (adapted from [38], and [21])

in CTTS and in absorption in WTTS (more similar to normal MS stars). The continuum level of some of the CTTS is higher than in normal stars. This means that a continuum component is superimposed to the stellar continuum. This additional component is called veiling and is not observed among WTTS. Finally, the Ca-II IR triplet on the red part of the spectrum is sometimes seen in emission in CTTS (e.g. [14]).

The spectrum of the Herbig Ae/Be stars is very similar to the CTTS ones with strong emission in the Balmer and metallic lines and occasional emission in the Ca II IR triplet. However, no veiling has been detected so far in HAeBe spectra [37, 40], and the Balmer jump is not seen in emission, but generally a smaller discontinuity is present than in normal stars of same spectral types (e.g. [39]).

In Fig. 7.3 the typical spectral energy distributions (SEDs) of CTT and HAeBe stars are shown. This plot represents the light flux in function of wavelength. The

squares, diamonds and crosses represent the observations obtained with photometric or low-spectral-resolution instrumentations. The dashed lines represent the predictions from models of stellar atmospheres calculated with suitable temperature in each example. Compared to a normal MS star, both CTT and HAeBe stars have strong IR-excess, and many times a silicate emission at 10 μm is observed. A "3 μm IR bump" is observed in the near-IR spectrum of many HAeBe stars, but never in TT stars (e.g. [32, 45]). On the blue side of the SED, an optical and UV excess is observed in CTT stars, while a UV depletion is sometimes observed in HAeBe stars.

The classical T Tauri stars can also be strongly photometric variable with amplitude of variability very different from one star to another, ranging from 0.1 to 2 mag. The variability is found irregular in most of the CTTS, but quasi-periodicity has been observed in the AATAU-type stars, called after their prototype AA Tau. In this sub-class of objects, the maximum flux is roughly at the same level, while the minimum flux is strongly varying from one cycle to another. The periods vary from 1 to 20 days (e.g. [16]).

The Herbig Ae/Be stars are usually not photometrically variable [47]. However a small portion is found to show strong drop of luminosity up to 3 mag. These UXOR stars have been named after their prototype UX Ori and concern only HAe stars. This drop in luminosity is accompanied with a blueing effect of the star that is not yet understood (e.g. [79, 82]).

The emission spectra of CTT and HAeBe stars are strongly variable. Hα can show sometimes double-picked emission, often associated with circumstellar disks, and sometimes P Cygni profiles, revealing winds in the close stellar environment (e.g. [6, 23]). Among the Herbig Ae objects, the spectral lines of the UXOR-type stars are superimposed with transient absorption components (TACs) highly variable that could be formed by circumstellar clouds (e.g. [44]). These variabilities are not found periodic, except in few Herbig Ae stars that show periodic features inside the Hα line profile (e.g. [22]).

Finally X-ray emission are very often detected from CTTS. These emission are highly variable with flares, and reveal hot plasma in the close environment (e.g. [50]). In the low-mass classical T Tauri stars the X-ray emission are believed to come from the magnetic activity present at the surface of the star. X-ray emission have only been firmly established coming from HAeBe stars in only a small number of them (e.g. [76]). While no correlation has been observed between the presence of X-rays and magnetic fields, their origin is still highly debated.

The characteristics of the CTTS and HAeBe stars summarised in this section reveal a complex structure and geometry surrounding the young stars that affect the full electromagnetic spectrum, from X-rays to IR, and even up to radio as we will see below. The following of this chapter will only concentrate on material from the disk which is cooler than material closer to the star and will therefore focus mainly on the stellar properties observed in the IR and at larger wavelength.

The aim of the following sections is to introduce the reader to what are called *accretion* disks, and what are our basic knowledge on the structure, composition and evolution of the disks. The paper does not aim to produce an exhaustive review on accretion disk, and I would redirect the reader to the following reviews for more

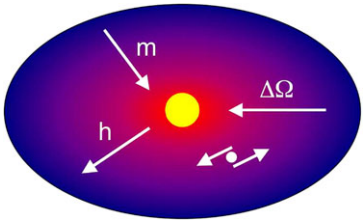

Fig. 7.4 Schematic representation of angular momentum and mass transport inside an accretion disk as described by Lynden-Bell and Pringle [59]

details on accretion/protoplanetary disks and on the recent work that has been done is this field: Williams and Cieza [84] for a global review on protoplanetary disks and their evolution, Dullemond and Monnier [33] for the inner region of the disks, Armitage [9] for the dynamics of disks, Zinnecker and Yorke [86] for massive star disks, van Dishoeck [80] for IR spectroscopy of gas and dust in the disks, Balbus [12] for the angular momentum transport in accretion disks, and Wyatt [85] for the final stages of protoplanetary disks.

7.2 Accretion Disk

7.2.1 Definition and Evidence

When the molecular cloud contracts to form a star because of the presence of angular momentum, the contraction will not be entirely spherical. While the central protostar grows roughly spherically by accreting matter from the envelope, the outer part of the cloud tends to be mainly distributed into a disk due to the action of the gravity and centrifugal forces. In presence of rotation the orbit of least energy is circular. The matter located in the disk is rotating with a Keplerian motion around the central star. The Keplerian angular velocity of a particle orbiting in the disk is given by

$$\Omega_{\rm K} = \left(\frac{GM_\star}{r^3}\right)^{1/2}, \tag{7.1}$$

where G is the universal gravitational constant, $M_\star$ is the mass of the star, and r is the distance between the centre of the star and the particle (see a schematic representation of the problem in Fig. 7.4). As a result, the angular velocity decreases outwards, while the specific angular momentum that scales as $h = r^2\Omega$ increases outwards (the specific angular momentum is the angular momentum per unit of mass). If the disk is viscous, the inner parts that are rotating faster than the outer parts shear past the outer parts. A transport of angular momentum is established from the inner part to the outer part. According to Lynden-Bell and Pringle [59], a simple energy balance shows that a viscous disk can lower its energy by transporting mass towards lower radius and angular momentum towards larger radius. The Keplerian disks surrounding young stars are therefore very likely accreting mass from the outer parts to the inner parts of the disk, while angular momentum is evacuated towards the outer part of the disk.

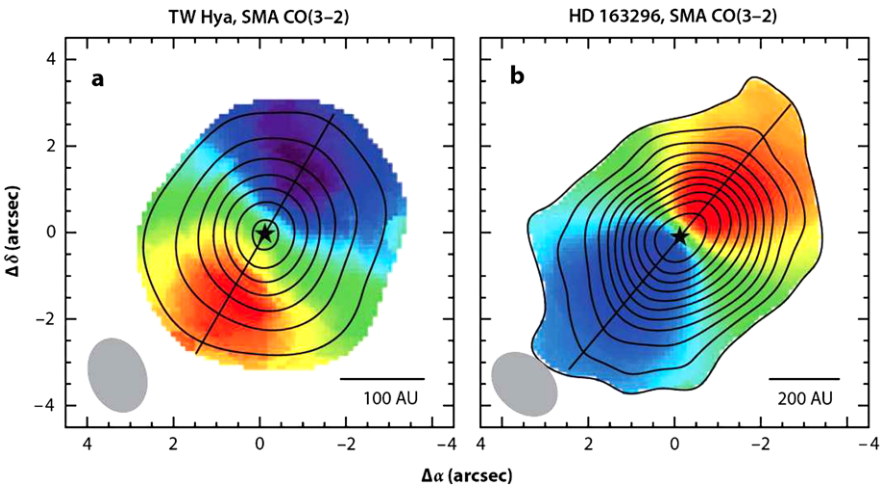

Fig. 7.5 CO(3–2) emission from the disk of the T Tauri star TW Hya (**a**) and the Herbig Ae star HD 163296 (**b**). The colors represent the velocity field of the gas with respect to us and show clearly matter coming towards us (*in blue*) and moving away from us (*red*) consistent with a Keplerian rotation of material in a disk that would be inclined with respect to the line of sight (from [84])

Evidence of material in Keplerian rotation within elongated structure has been obtained by many authors by measuring the radio emission from the molecular gas in the environments of young stars (Fig. 7.5, see also [61]). Evidence of hot disks has also been obtained using various observing techniques such as coronography (e.g. [10, 41]), adaptive optic (e.g. [69]), interferometry [35], or IR imagery (e.g. [43, 68]). From these observations it seems now evident that the material situated from small AU to large AU is distributed into a disk.

7.2.2 The Disk Structure and Composition

7.2.2.1 Passive Versus Accretion Disks

One of the first models of accretion disk has been proposed by Lynden-Bell and Pringle [59] to understand the evolution of viscous disks surrounding stars. They propose that in such Keplarian viscous disks the dissipation lead to shining. The light emitted from the disk can be divided in two components: from the disc itself radiating energy at a temperature that varies with the distance from the central star and a boundary layer that is heated by the interaction of the inner part of the disk and the surface of the star. This "boundary-layer model" was predicting the presence of IR excess and UV excess, as observed in many T Tauri stars.

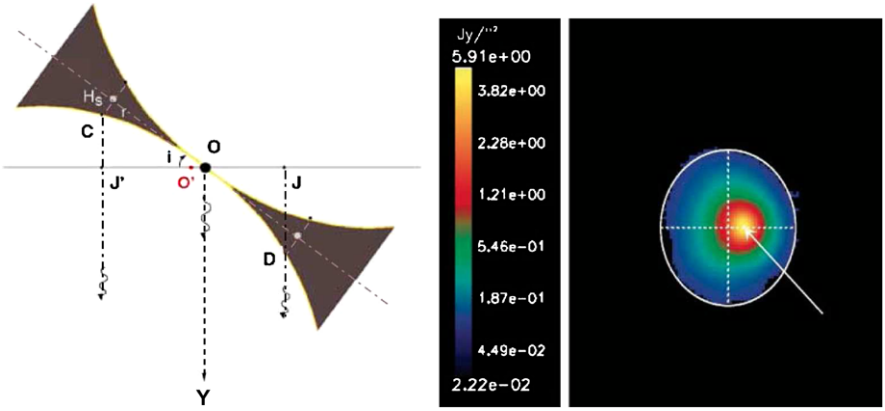

Fig. 7.6 *Left*: Schematic of the flared disk of HD 97048. The disk is seen from below with an inclination i between the line of sight and the disk axis. C and D are two points situated at the surface of the disk and at the same distance from the star (in O). Due to geometrical effect, we expect the centre of emission from C and D to be in O' that is offset from the geometrical center O. *Right*: IR observation of the disk around HD 97048. The photo-centre of the IR emission (indicated by the *arrow*) does not coincide with the geometrical center of the image (surrounded by a *white ellipse*) as was predicting the sketch of the left panel (from [57])

Many authors used this initial idea to reproduce the SED of T Tauri stars and in particular the IR slope of the SED. Adams et al. [2] defined the spectral indices as

$$n = -\frac{d \log \lambda F_\lambda}{d \log \lambda}, \tag{7.2}$$

where λ is the wavelength, and F_λ is the flux from the object. n is evaluated in the near- to mid-IR portion of the spectrum (i.e. $\lambda \sim 1$–10 μm). The classical T Tauri stars present typical spectral indices from $4/3$ to nearly 0 (flat IR spectrum). A classical Keplerian accretion disk as proposed by Lynden-Bell and Pringle [59] predicts a spectral index of $4/3$. On the other hand, Adams et al. [2] showed that a "passive" disk (i.e. without accretion and therefore viscous dissipation) with the reprocessing of about 25 % of the stellar light being the only source of energy, can also produce a flux with a spectral index of $4/3$.

7.2.2.2 The Flaring Disk

The spectral indices of T Tauri stars are mostly found to be higher than $4/3$, implying that an additional source to the viscous accretion or to the light reprocessing has to be present. Kenyon and Hartmann [53] show that a flat IR spectrum can be reproduced with a passive reprocessing disk if it flares slightly as radial distance increases (Fig. 7.6, left). They argue that if the disk is optically thick, reprocessing must exist and therefore a significant fraction of the IR emission has to come from reprocessing. A disk in hydrostatic equilibrium tends to flare: in the direction perpendicular to the mid-plane of the disk, the component of the gravitational force of

the star is balanced by the gas pressure gradient. So in the disk, at a radius r from the centre of the star and at a distance z above the mid-plane, the pressure of the gas (p) is given by

$$\frac{dp}{p} = \frac{\Omega_{\rm K}^2}{v_{\rm s}^2} z\, dz, \tag{7.3}$$

where $v_{\rm s}$ is the speed of sound, and $\Omega_{\rm K}$ is the Keplerian angular velocity as defined before. From this equation we can derive the scale height of the disk (e.g. Kenyon and Hartman 1987):

$$\frac{h}{r} = \left(\frac{v_{\rm s}^2 r}{G M_\star} \right)^{1/2}. \tag{7.4}$$

If the internal temperature of the disk $T_{\rm int}(r) \propto v_{\rm s}^2$ falls off more slowly than r^{-1}, then the relative thickness of the disk will increase outwards: the surface of the disk is therefore concave. The predicted internal disk temperature of passive reprocessing or active accretion flat disks is $T_{\rm int}(r) \propto r^{-3/4}$ [2, 59]. If the disk is vertically isothermal, the surface temperature ($T_{\rm s}$) should have the same temperature as the interior, and the scale height would be proportional to $r^{1/8}$, which makes the flared disk a plausible hypothesis.

A protostellar disk is composed of gas and dust with a ratio of about 100:1 in mass (assumed similar to the interstellar medium). While the flaring structure is supported by the gas, the dust is absorbing and reemitting the stellar light. In the case of a vertically isothermal disk with dust well mixed with the gas, Kenyon and Hartmann find that the effective height $H_{\rm s}(r)$ of the disk is about $3h$. More recent models give $H_{\rm s}(r) \sim 4h$ (e.g. [27]). $H_{\rm s}(r)$ can therefore be written as the power law $H_{\rm s}(r) = H_0(r/R_\star)^z$, where $z = (3-\gamma)/2$, and where γ is defined as $T_{\rm s}(r) \propto r^{-\gamma}$. If optically thick, a flared disk will intercept a larger fraction of the stellar radiation than a completely flat disk. Kenyon and Hartmann find that for a temperature distribution $T_{\rm s}(r) \propto r^{-1/2}$, about 50 % of the stellar light is reprocessed and can reproduce flat IR spectrum as observed in the most extreme T Tauri stars. However, Adams et al. [3] argue that because of vertical dust settling within the disk, Kenyon and Hartmann overestimate the reprocessing efficiency, and in order to reproduce their large-IR excess and reach a temperature distribution of $T_{\rm s}(r) \propto r^{-1/2}$, an additional non-viscous activity within the disk must be present.

7.2.2.3 The Two-Layer Model

Calvet et al. [19, 20] performed more detailed calculation of a steady, viscous, geometrically thin, optically thick flared accretion disk. In their models they assume that the internal energy of the disk has both sources, the irradiation from the star and accretion. The outer layers of the disk form an atmosphere, and the disk structure is therefore the combination of an optically thick viscous disk with an optically thin non-viscous atmosphere in radiative equilibrium. The atmosphere is irradiated by the star, which absorbs a fraction of the stellar flux and scatter the other fraction.

Its temperature is determined by heating from the viscous interior and the stellar radiation absorption as it travels down the atmosphere. They find that the irradiated disk dominates the flux at wavelength larger than 1 μm whatever the stellar effective temperature or the mass accretion rate inside the disk.

They performed radiative transfer inside the atmosphere by including specific electronic, vibrational and rotational transitions of molecular and atomic elements (H, H_2, C, Si, Mg, CO, TiO, OH, H_2O and silicate) that are assumed to be the main source of opacity in the near- and mid-IR. They find that the spectral signatures of CO and TiO, and the silicate feature at 10 μm is strongly dependent on the mass accretion rate and the stellar effective temperature, as the former affects the viscous energy injected into the atmosphere and the latter affects the amount of radiation heating the atmosphere. These features are formed at low optical depth in the upper layer of the atmosphere mostly affected by the stellar radiation: the lower the accretion rate and the higher the stellar temperature, the more these features appear in emission. For high accretion rate and low stellar temperature, they would appear in absorption. Therefore Calvet et al. propose that the observation of these features would give an indication on the accretion rate inside the disk.

7.2.2.4 The Disk Inner Gap

Chiang and Goldreich [25, 26] investigate the case of a passive disk in hydrostatic and radiative equilibrium. Their calculations are similar to those performed by Calvet et al., except that the optically thick disk interior is heated by the radiation of the stellar light reemitted by the dust grains in the surface layer. The dust absorbing the incident stellar ration radiates equal amounts of IR radiation into the inward (the disk interior) and outward hemispheres. Their models aim to reproduce the nearly flat mid- to far-IR spectrum of T Tauri stars. Their models allowed the line-of-sight inclination angle to vary, and they argue that due to the flaring if the inclination is high (the disk is seen near equator-on), the outer part of the disk could occult the inner regions and reduce significantly the flux shortward 30 μm, and could explain the lack of IR emission around 12 μm observed in many T Tauri stars. From the fitting of the SED of the stars their model derives the inclination angle, the surface density of the disk, the emissivity of the grains, their typical size, and the inner and outer radii of the disk. Figure 7.7 shows the result of the fit of the SED of the T Tauri star GM Aur. They find that even with a inclined disk, the disk must be truncated between the star and the inner rim of the disk up to 4.8 AU, which is about 60 times larger than the dust sublimation radius (radius below which the temperature is too high for the dust to persist). They therefore cast some doubt about the reality of such a large gap in the centre of the disk. Inner holes are also required in disks around Herbig Ae/Be stars but with a much smaller size. Hillenbrand et al. [51] have fitted the SED of group I Herbig Ae/Be stars (i.e. stars with spectral indices of 4/3) with an optically thick, geometrically flat accretion disk. They can well reproduce the spectral shape of these stars under the condition that the inner part of the radius (shortward 2.2 μm, i.e. few stellar radii) is optically thin. Lada and

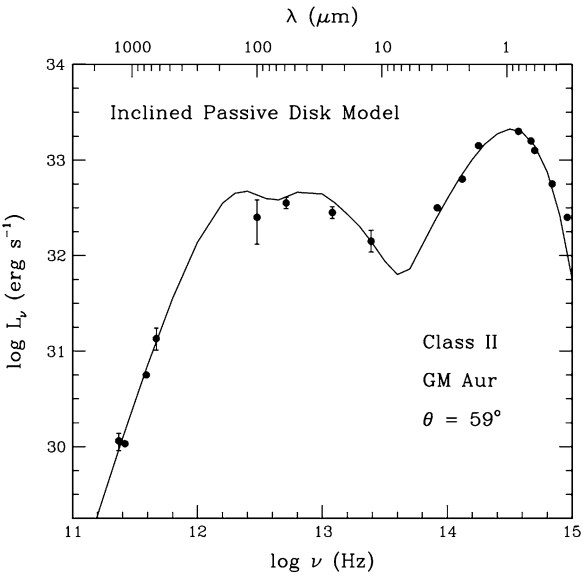

Fig. 7.7 Observed SED (*filled circles*) of the T Tauri star GM Aur superimposed with the inclined passive disk model (*full line*). The best disk model has been found with an inner edge at 4.8 AU, an outer edge at 311 AU, and an inclination angle of 59° (from [26]). Note that the x-axis is in frequency (and not in wavelength as generally found in the literature)

Adams [56] reach the same conclusion by studying the distribution of HAeBe stars in the *JHK* infrared color–color diagram. In particular, they find that to reproduce the observations, the inner edges of the disk should have temperature between 2000 and 3000 K, close to the dust sublimation temperature.

7.2.2.5 Evidence of Grain Growth

D'Alessio et al. [29, 30] have developped models of irradiated accretion disks. The disk is assumed to be geometrically thin and in steady state with a constant mass accretion rate and in vertical hydrostatic equilibrium. The disk is heated by viscous dissipation, radioactive decay, cosmic rays and stellar radiation. They find that the irradiation from the central star is the main source of heating of the disk except in the innermost regions, within ∼2 AU from the central star, where the stellar light has a grazing incidence, and hence the viscous dissipation is the dominant source of heating. They used their model to fit the SEDs of a large sample of T Tauri stars. Their model can well reproduce the observed near-IR fluxes, but they predict fluxes that are too high at far-IR and too low at millimeter wavelength (Fig. 7.8, upper left), indicating that their model is too geometrically thick at large radii. They propose that dust settling and coagulation could have already occurred, which would reduce the geometrical thickness of the disk. D'Alessio et al. [28] allowed in their models dust grain growth with power-law size distributions, such as the size distribution of dust grains is given by $n(a) = n_0 a^{-p}$, where a is the size of the grains, n_0 is the normalisation constant, and p is a free parameter. They find that compared to models with a dust disk composition similar to the interstellar medium (assumed similar to the dust composition of molecular clouds), their models reduce the vertical dust

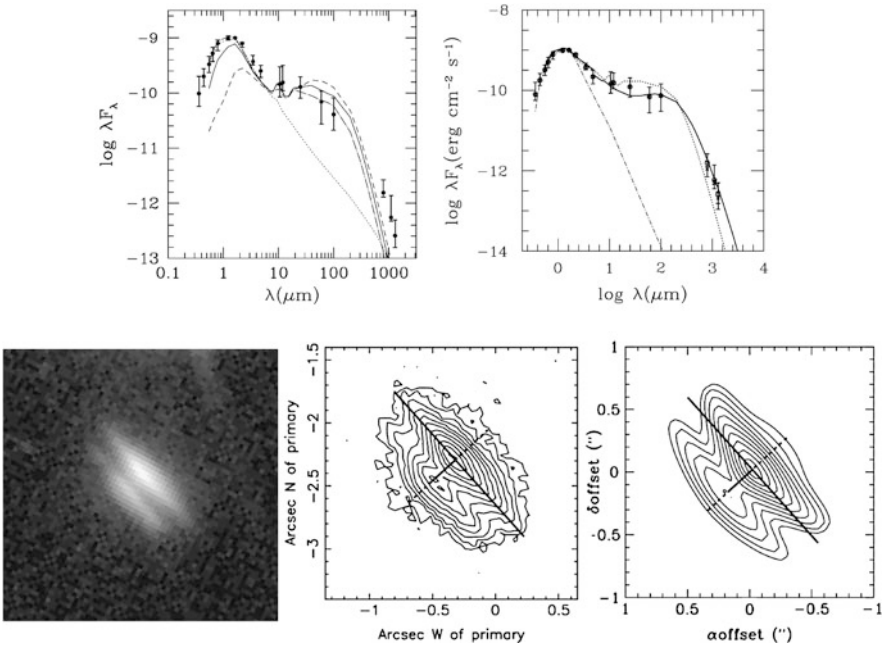

Fig. 7.8 This group of figures illustrates the necessity to take into account a non-uniform distribution of grain sizes in models of disk in order to better reproduce the observations. *Upper left*: The median observed SED (*filled circle*) of the PMS stars of the Taurus-Aurigae molecular cloud superimposed with the models of D'Alessio et al. [29] of three different disk radii assuming grains distribution similar to the interstellar medium (ISM). Whatever the disk size, they cannot reproduce at the same time the far-IR and mm observations (from [29]). *Upper right*: The *circles* are the same data point as in the left panel. The *dot-dashed line* is the photospheric spectrum. The *dotted-line* is the ISM-dust model, while the *solid line* is a dust model that allowed the dust distribution to vary as a power law with $p = 3.5$ (see text) and a maximum grain size of 1 mm. This model is capable of a better agreement between the far-IR and mm observations of T Tauri stars (from [28]). *Bottom left and middle*: *Hubble Space Telescope* (*HST*) visible image of the companion to HK Tau, designed as HK Tau/c, and its surface brightness map (from [73]). *Bottom right*: Surface brightness map of a disk model [28]. Note the strong similarities between the observations (*bottom middle*) and the model (*bottom right*)

height, and hence the irradiation heating is reduced, while the emission of the disk at mm and submillimeter wavelengths is enhanced. This model agrees better with the SEDs and IR imaging of T Tauris stars (Fig. 7.8, upper right and bottom).

7.2.2.6 Dust Composition

Chiang et al. [27] improved their model of passive disk by accounting a range of particle sizes as a function of grain nature and therefore as a function of local temperature. Figure 7.9 (upper right) is a schematic representation of the disk showing the zones of grain composition. In their model, Chiang et al. have limited the com-

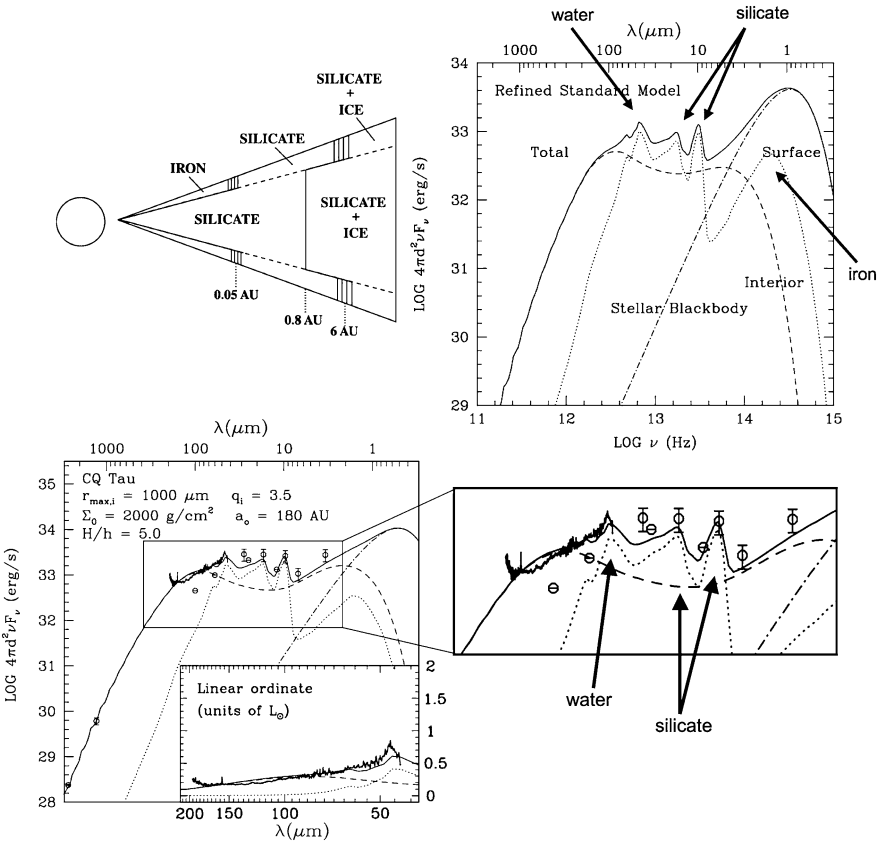

Fig. 7.9 *Upper left*: Schematic of zones of grain composition in the interior and in the atmosphere of the disk as computed in the models of Chiang et al. [27]. *Upper right*: Modelled SED of a passive disk taking into account a range of particle sizes (*solid line*). The water and silicate features are easily identifiable. However, the iron feature is lost in the stellar photospheric spectrum. The different contribution to the total SED from the stellar photosphere, the disk interior and the disk atmosphere are plotted with broken lines. (Note that the flux is plotted as a function of frequency and not wavelength.) *Bottom*: In the *left panel* there is plotted the SED of the Herbig Ae star CQ Tau superimposed with the best-fit model of Chiang et al. [27]. A close-up view is shown in the *right panel*. The water and silicate features are detected in this star (adapted from [27])

putation to only three types of grains: metallic iron, amorphous olivine (silicate) and water ice. They have tested that these grains are dominating the disk physical processes at temperature going from about 100 to 2000 K. In their models, where the local dust temperatures (that is assumed similar to the gas temperature) are lower than ∼150 K (that is the water ice sublimation temperature, and corresponds to a distance from a typical T Tauri star of about 6 AU in the atmosphere of the disk and 0.8 AU in the interior of the disk), the grains are mainly silicate covered with water ice. At temperature between ∼150 K and ∼1500 K (the silicate sublimation temperature, corresponding to ∼0.05 AU in the atmosphere and ∼2 R_* in the interior),

they assume that the grains are mainly silicate only. Finally, between 1500 K and 2000 K (the iron sublimation temperature, corresponding to $\sim 2\ R_*$), the grains are mainly iron.

In Fig. 7.9 (upper right) we see the detailed relative contribution from the stellar blackbody, the disk interior and the disk surface emissions to the total SED of T Tauri stars as predicted by the models of Chiang et al. They find that two emission features from the silicate could be detected at 10 and 18 μm, and water ice features could also be observed at 45 and 62 μm. A dearth of emission between 2 and 8 μm from the silicate is predicted and explained by the fact that the silicate grains have a typical size lower than 1 μm and are therefore transparent at these wavelengths. Chiang et al. [27] used their models to fit the IR spectra of two T Tauri and three Herbig Ae stars from the Long-Wave-Spectrometer (LWS, 43–195 μm) onboard the Infrared Space Observatory (ESO). They were able to identify the water feature at 45 μm and both silicate features as predicted by their models, in both T Tauri stars and in the coldest Herbig Ae star considered in their study. No evidence of water could be found in the ISO spectra of the two hottest Herbig Ae stars. Later, using data from the Spitzer Infrared Spectrometer onboard the space telescope Spitzer, Pontoppidan et al. [71] were not able to find evidence of water in the spectra of the 25 A or B stars of their sample, while more than half of the late-type (M-K) stars have detectable water emission. This suggests that the temperature of the central star has a strong impact on the excitation and/or chemistry at the surface of the disks. On the other side, evidence of polycyclic aromatic hydrocarbons (PAHs) has been observed in the IR spectrum of many Herbig Ae/Be stars, but not in T Tauri stars. The PAHs bands are excited by the UV radiation from the star and explain why they are found stronger in the most massive stars and are absent in T Tauri stars. Besides amorphous silicate, crystalline silicates are also found in Herbig Ae/Be stars. However, no correlation with age has been found, and it is not clear what is the origin of these crystalline silicates and what are their evolution with the age.

7.2.2.7 The Puffed-Up Inner Rim

While the models detailed in the previous sections have been mainly developed for low-mass T Tauri stars, they have been relatively successfully applied to Herbig Ae/Be stars, and it is now evident that the IR excess observed in these objects is emitted by their dusty disks. However, one of the characteristics of the SED, specific to Herbig Ae/Be stars, is still difficult to interpret with the simple models described above: the near-IR or "3 μm bump", characterised by an inflection of the SED at wavelength shortwards ~ 2.2 μm.

Hillenbrand et al. [51] were able to fit the SED of HAeBe stars using a non-irradiated geometrically-flat, optically thick disks with a very large accretion rate, and an optically thin inner hole. However Hartmann et al. [45] argue that an optically thin inner disk is inconsistent with a large accretion rate. Instead, they propose that the NIR excess emission originates from a dusty circumstellar envelope containing very small grains transiently heated by the UV flux of the star. However, this

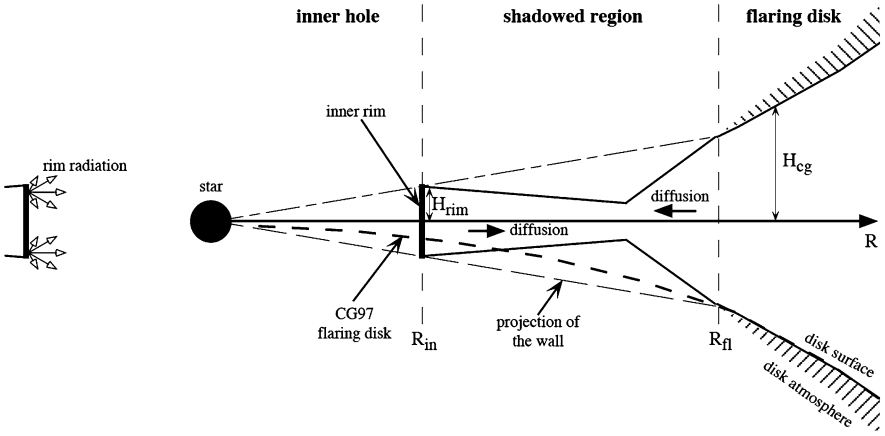

Fig. 7.10 Schematic representing the formation of the puffed-up inner rim, the shadowed region right behind the rim and the remaining flaring disk not shadowed by the rim (from [32])

hypothesis has been ruled out for theoretical [66] and observational reasons [62]. Natta et al. [67] proposed instead a model of passive flared disk with an optically thin inner hole. As the dust sublimation temperature is around 2000 K, corresponding to few stellar radii, the inner part of the disk is naturally depleted of dust. The inner rim of the disk is therefore directly irradiated by the star and is therefore hotter than what would be a full flared disk at the same radii (close to the star, below $\sim$1 AU, the stellar light irradiates the disk with a grazing angle). As the rim is hotter, its vertical scale increases, and it puffs up. This hot inner wall could explain the near-IR bump observed in many Herbig Ae/Be stars. Dullemond et al. [32] go further and try to understand the impact of the presence of this inner wall to the rest of the disk. In particular, they investigate the impact of the shadow of the rim to the rest of the flaring disk. The shadowed region can cover a large part of the disk, and in some cases the whole disk could reside inside the shadow. Therefore, in some cases the 10 μm silicate feature could disappear, which would explain its absence in some of the HAeBe SEDs [62]. In the other cases, the part of the disk that is directly illuminated by the star continues to flare and to be mainly heated by the stellar radiation. In Fig. 7.10 the models proposed by Dullemond et al. [32] are schematically represented. In a self-shadowed disk, the disk is not irradiated by the central star anymore, and therefore the evidence of PAHs in the stellar spectra should be strongly reduced. The ISO spectra analysis of 46 HAeBe stars performed by Acke and van den Ancker [1] confirm these expectations.

Recent observational evidence of inner hole have been obtained recently [42, 63] in Herbig Ae/Be stars. Furthermore, the recent determination of mass accretion rate in Herbig Ae/Be stars revealed values that are sufficiently low to ensure an optically thin inner gaseous disk at radii shorter than the dust sublimation radius. These results are therefore in agreement with the Dullemond et al. model.

7.2.2.8 The Inner Disk Warp of Classical T Tauri Stars

As presented in Sect. 7.1.3, a sub-class of classical T Tauri stars present cyclic photometric variability, the AATAU-type stars. Bouvier et al. have deeply studied the spectroscopic, photometric and polarimetric characteristics of their prototype and proposed a model that can explain all of them. Bouvier et al. [17] have found that the photometric light-curve of AA Tau displays a constant brightness interrupted by quasi-cyclical drops. The drops can change in shape and duration from one cycle to another but regularly appear every 8.2 days. They also observe that the veiling increases and the polarisation is larger when the star faints. The low-mass CTT stars can develop magnetic fields at their surface and experience magnetospheric accretion. The large-scale magnetic field of AA Tau is similar to an inclined dipole that disrupts the inner part of the disk to form a magnetosphere. The matter from the inner part of the disk is channeled along the field lines to reach the surface of the star close to the magnetic pole, where accretion shocks are formed, which are causing the veiling largely observed among T Tauri stars. Bouvier et al. propose that the interaction of the magnetic fields with the inner part of the disk causes the part of the disk that is closer to the magnetic pole (i.e. where the magnetic field is more intense) to wrap. A schematic representation of their model is presented in Fig. 7.11. As the star is seen nearly edge-on, the wrap crosses the line of sight and fades the star regularly as the star rotates. The polarisation is therefore increasing as a larger quantity of material is scattering the stellar light during fading events, and the veiling also increases as the stellar spots face us during the fading events.

The system AA Tau experiences some quiescent episode during which the fading disappears. Bouvier et al. [18] argue that it is the result of the dynamic of the magnetic field of AA Tau that can be temporarily disrupted. The magnetosphere of the star extends from the stellar surface to the inner edge of the disk that is rotating with a Keplerian velocity different from the stellar rotation velocity. The differential rotation from the foot-points of the magnetic field lines that are anchored in the stellar surface on one side and in the inner edge of the disk on the other side could shear the field lines until it reaches a critical point where disruption occurs. After few cycles, the large-scale magnetic field is reconstructed with or without the same configuration as before the disruption. The difference observed from one drop to another is the result of a combination of the dynamic interaction of the magnetic field with the disk, of the dynamical movement inside the disk, and of the dynamical distortion that the magnetic fields experience inside the magnetosphere.

AA Tau seems to not be a peculiar object. Recent observations of the satellite CoRoT that aims at observing the same field of the sky for long time, and compiling light-curve of many objects obtained on many successive months without interruption, have revealed many AATAU-type light-curves in the very young cluster NGC 2264 [7]. This is a very nice confirmation that high dynamical processes are acting in very young star-disk systems and play an important role on the shaping of the magnetosphere and the inner part of the disk.

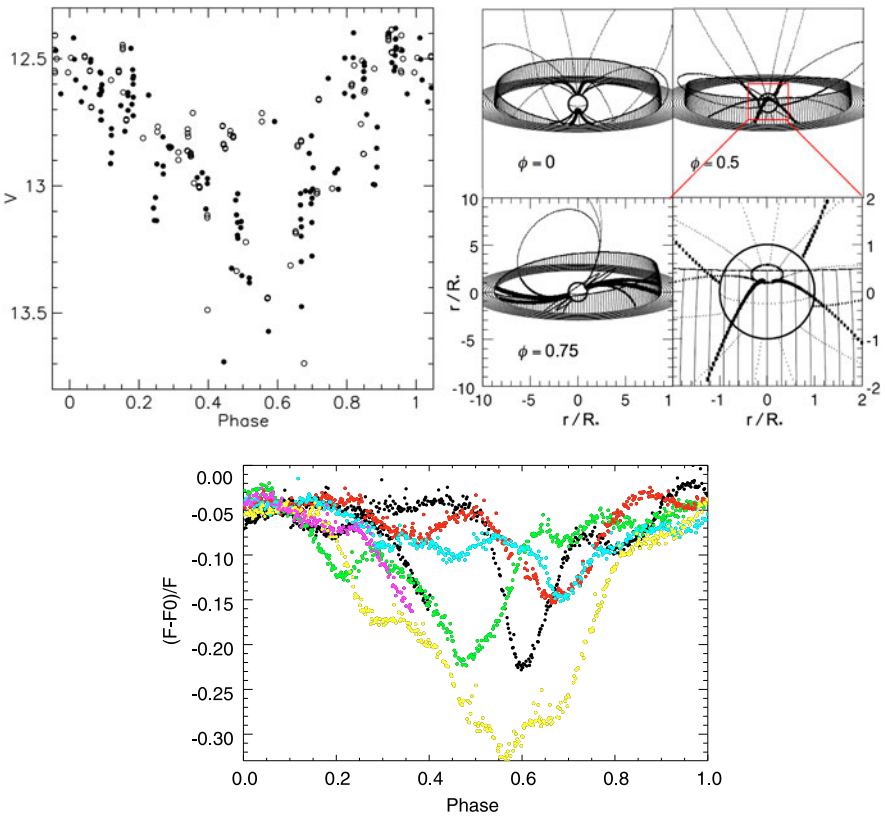

Fig. 7.11 *Upper left*: AA Tau light-curve folded in phase. The different symbols represent different cycles (from [17]). *Upper right*: Illustration of the model of the inner disk wrap proposed to explain the light variations of AATAU-type stars. *Three panels* represent the star-disk system at three different rotation phases (0., 0.5, 0.75). The *last panel* is a close-up view of the panel at phase = 0.5 (from [17]). *Bottom*: CoRoT light-curve folded in phase for one of the AATAU-type NGC 2264 star. The different colors represent different cycles (from [7])

7.2.2.9 Clumpiness of the Near-Stellar HAe Dust

Among the Herbig Ae stars, a sub-class shows very strong photometric variability. These stars are called the UXOR objects. These objects show in their spectra transient absorption components (TACs) that consist in absorption lines superimposed with the photospheric lines that appear and disappear within few days (see Fig. 7.12, left, [64, 65]). These TACs are observed in Balmer lines and metallic lines as well. These TACs reveal the presence of clumps of dust and gas that cross the line of sight. It is believed that these clumps are formed from hydrodynamical fluctuations inside the disk. If the disk is viewed close to edge-one, then the manifestation is therefore observable through photometry and spectroscopy. At lower inclination, no evidence of these clumps can be detected, which explains why the UXOR phenom-

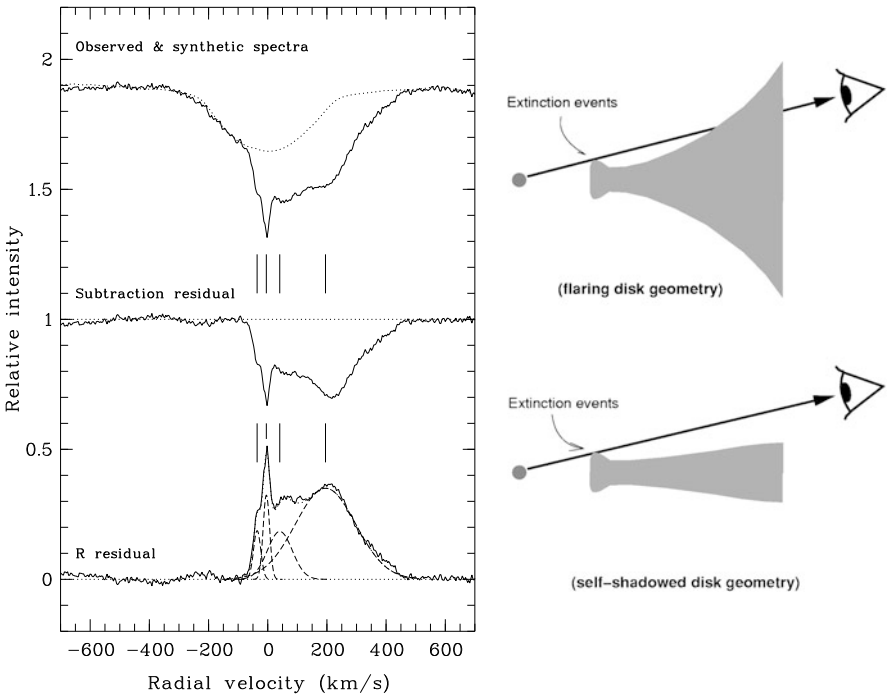

Fig. 7.12 *Left*: Illustration of the transient absorption components (TACs) observed in UXOR type star. *On the top* there is represented the Ca II K line as observed in the spectrum of UX Ori. The predicted photospheric line profile is overplotted with a *dotted line*. *In the middle* the predicted photospheric profile has been subtracted to the whole profile. *At the bottom* the normalised residual ($R = 1$—observed/photospheric) is plotted. The four individual TACs have been identified with *dashed lines* (from [65]). *Right*: Illustration of the nearly-edge one Dullemond et al. model. *On the top* is represented a flaring disk that is obscuring the star and the inner edge of disk, forbidding the observer to detect the fading events of UXOR-type stars. *In the bottom*, a self-shadowed disk seen nearly edge-on could exhibit these events to the observer (from [34])

ena are observed only in a small fraction of the Herbig Ae stars. Dullemond et al. [34] argue that their model of puffed-up inner rim that shadows the disk can explain how these blobs are observable. They explain that if the disk is flaring and the disk is seen near edge-on, with an inclination that allows the clumps to cross the line of sight, the outer part of the disk would occult the star. However, in the case of self-shadowed disks, with an edge-on inclination the inner part of the disk where the blobs are formed can be aligned with the line of sight (Fig. 7.12, right).

Other hypotheses have been proposed to explain the UXOR phenomena, such as an occulting screen that would occult the star and the close circumstellar gas, or magnetospheric accretion, or gaseous evaporation bodies [15, 64, 72]. A combination of some of these theories could also be possible. Many more observations and models need to be performed in order to fully understand the origin of the UXOR phenomenon.

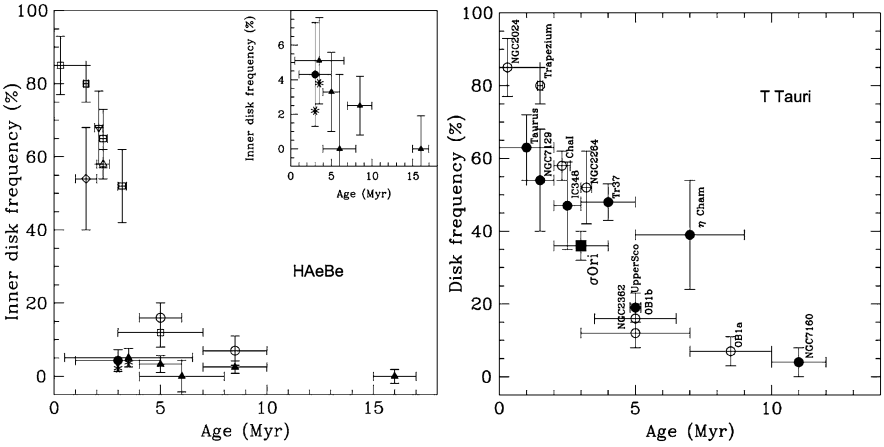

Fig. 7.13 *Left*: Inner disk frequency of HAeBe stars in nearby OB association as a function of age (from [49]). *Right*: Disk frequency of T Tauri stars of young clusters and associations (from [48])

7.2.3 The Disk Evolution

The observation of very young OB associations, where sequential formation occurred, revealed that in low-mass T Tauri star the disk frequency is dependent on the age suggesting a disk lifetime around 10 Myr. In the more massive Herbig Ae/Be star the lifetime is even reduced to about 5 Myr ([31, 48–50], Fig. 7.13). Hernandez et al. [49] find that the inner disk is disappearing faster than the outer part with a lifetime for the inner part that is around 3 Myr for Herbig Ae/Be stars.

Central holes, nearly devoid of dust, have been inferred from IR observations in the disks of T Tauri and Herbig Ae/Be stars with sizes of the order of 10 AU, i.e. much larger than the dust sublimation radius (e.g. [36, 54, 74, 78]). These disks are found around stars that are slightly older than stars surrounded with full dusty disks and that are younger than the young main-sequence stars surrounded with debris disk (Vega-like stars [11]). These disks are therefore assumed to be a transitional phase between accretion disk and debris disk and are called *transitional* disks.

These results suggest that the disk clearing process is from inside to out. There exist many theories of clearing processes that could explain that the inner part of the dusty disk disappear before the outer part. Weidenschilling [83] has shown that the growth of grains by coagulation (due to Brownian motion, turbulence and settling in the high-density internal disk) is faster in the inner disk than in the outer disk. If grains grow in the inner part, the opacity at short wavelengths decreases, which would explain the lack of near-IR excess in transitional disks. Another explanation is the formation of a planet. A planet of high-enough mass can clear its surrounding via torque and create a gap that will progressively extend up to the surface of the star to produce an inner hole as observed. The gap and the hole would be the result of an enhanced angular moment transport and accretion induced by spiral waves (e.g. [81]). Magneto-rotational instability (MRI) has also been proposed to explain

the disk clearing. The stellar X-rays would ionise the disk. A surface layer would be formed and well coupled with the inertial magnetic field of the disk. MRI would therefore be activated, and either a disk wind or a enhanced accretion would allow the gas and dust to leave the disk [24, 75]. Finally, photoevaporation could also explain the disk clearing from inside to outside. The UV radiation field of the star ionise the outer part flaring disk (where the incident angle is higher). Above a critical radius, the matter leaves the disk through an evaporating wind. The mass accretion rate inside the disk decreases with time. At one point it reaches a value smaller than the mass loss rate of the evaporating wind. The outer part is not able anymore to replenish the inner part of the disk that continuously accretes matter onto the star until it is emptied. When the inner disk disappears within about 10^5 years, the ionising stellar radiation can penetrate the outer part of the disk, and about 10^5 years later the gas in the whole disk is lost by photoevaporation [8].

There is not yet any favoured scenario for the clearing of circumstellar disk. A combination of many of those presented here is certainly possible. Evidence of dust coagulation has been obtained in many disks (e.g. [58]), and (proto)planets have been detected in the transitional disk of young stars (e.g. [55]). It is generally believed that the natural evolution of the dust inside an accretion disk is to grow to form large grains that will continue to grow to form planetesimals and then planets. The question that still needs to be answered is whether these processes play an important role in the disk clearing. MRI could also play an important role but only in low-mass T Tauri stars as X-rays are required. In low-mass stars, X-rays are produced by the dynamo activity at the surface of the star, which is absent in higher-mass stars. On the contrary, the stellar UV flux increases with the stellar mass, which would favour the photoevaporation scenario for the Herbig Ae/Be star.

7.3 Conclusion

Today, most of the scientific community is convinced that the circumstellar gas and dust of the Herbig Ae/Be and T Tauri stars are mainly distributed into a disk. We did not discuss winds in this paper, but evidence of winds is also largely found in HAeBe and TT stars. The environments of class II stars is therefore mainly constituted of winds and disks. From theoretical and observational evidences it is very likely that the disks are flaring, at least in the low-mass stars were the UV radiation field is too low to photoevaporate the disk, and at least at one point during the history of the accretion disk. It appears from many theories that the irradiation from the star is the main source of energy. In T Tauri stars there is observational evidence that matter is accreted from the inner part of the disk to the stellar surface. The inner part of the disk must therefore be replenished, which implies accretion within the disk. Accretion is therefore likely occurring in the inner part of the disk; however, it is very difficult to access to observational indices from that part of the disk. In the case of Herbig Ae/Be stars, accretion is not so evident. Magnetospheric accretion is absent, and we can therefore wonder if accretion from the inner part of the disk to

the stellar surface is really happening. More work needs to be done to answer this question.

Most of our knowledge on the properties of accretion disks reside on the analyses of the SED of the star, which is a great tool but not sufficient to fully understand the physics of the disk. Recent works using multi-wavelength and multi-techniques of observations allowed a big step in our knowledge of the disks surrounding young stars (e.g. [70]). The new generation of instruments on the VLTI and the recent launch of the spatial telescope Herschel will bring new tremendous observational constraints that will challenge the disk theories and motivate new ones.

Acknowledgements I acknowledge financial support from "Programme National de Physique Stellaire" (PNPS) of CNRS/INSU, France.

References

1. Acke, B., van den Ancker, M.E.: Astron. Astrophys. **426**, 151 (2004)
2. Adams, F.C., Lada, C.J., Shu, F.H.: Astrophys. J. **312**, 788 (1987)
3. Adams, F.C., Lada, C.J., Shu, F.H.: Astrophys. J. **326**, 865 (1988)
4. Alecian, E., Wade, G.A., Catala, C., et al.: Mon. Not. R. Astron. Soc. (2012, submitted)
5. Alecian, E., Wade, G.A., Catala, C., et al.: Mon. Not. R. Astron. Soc. (2012, submitted)
6. Alencar, S.H.P., Johns-Krull, C.M., Basri, G.: Astron. J. **122**, 3335 (2001)
7. Alencar, S.H.P., Teixeira, P.S., Guimarães, M.M., et al.: Astron. Astrophys. **519**, A88 (2010)
8. Alexander, R.D., Clarke, C.J., Pringle, J.E.: Mon. Not. R. Astron. Soc. **369**, 229 (2006)
9. Armitage, P.J.: Annu. Rev. Astron. Astrophys. **49**, 195 (2011)
10. Augereau, J.C., Lagrange, A.M., Mouillet, D., Ménard, F.: Astron. Astrophys. **365**, 78 (2001)
11. Backman, D.E., Paresce, F.: In: Levy, E.H., Lunine, J.I. (eds.) Protostars and Planets III, pp. 1253–1304 (1993)
12. Balbus, S.A.: Annu. Rev. Astron. Astrophys. **41**, 555 (2003)
13. Behrend, R., Maeder, A.: Astron. Astrophys. **373**, 190 (2001)
14. Bertout, C.: Annu. Rev. Astron. Astrophys. **27**, 351 (1989)
15. Beust, H., Karmann, C., Lagrange, A.-M.: Astron. Astrophys. **366**, 945 (2001)
16. Bouvier, J., Alencar, S.H.P., Boutelier, T., et al.: Astron. Astrophys. **463**, 1017 (2007)
17. Bouvier, J., Chelli, A., Allain, S., et al.: Astron. Astrophys. **349**, 619 (1999)
18. Bouvier, J., Grankin, K.N., Alencar, S.H.P., et al.: Astron. Astrophys. **409**, 169 (2003)
19. Calvet, N., Magris, G.C., Patino, A., D'Alessio, P.: Rev. Mex. Astron. Astrofís. **24**, 27 (1992)
20. Calvet, N., Patino, A., Magris, G.C., D'Alessio, P.: Astrophys. J. **380**, 617 (1991)
21. Catala, C.: In: Reipurth, B. (ed.) European Southern Observatory Conference and Workshop Proceedings, vol. 33, pp. 471–489 (1989)
22. Catala, C., Donati, J.F., Böhm, T., Landstreet, J., Henrichs, H.F.: Astron. Astrophys. **345**, 884 (1999)
23. Catala, C., Felenbok, P., Czarny, J., Talavera, A., Boesgaard, A.M.: Astrophys. J. **308**, 791 (1986)
24. Chiang, E., Murray-Clay, R.: Nat. Phys. **3**, 604 (2007)
25. Chiang, E.I., Goldreich, P.: Astrophys. J. **490**, 368 (1997)
26. Chiang, E.I., Goldreich, P.: Astrophys. J. **519**, 279 (1999)
27. Chiang, E.I., Joung, M.K., Creech-Eakman, M.J., et al.: Astrophys. J. **547**, 1077 (2001)
28. D'Alessio, P., Calvet, N., Hartmann, L.: Astrophys. J. **553**, 321 (2001)
29. D'Alessio, P., Calvet, N., Hartmann, L., Lizano, S., Cantó, J.: Astrophys. J. **527**, 893 (1999)
30. D'Alessio, P., Canto, J., Calvet, N., Lizano, S.: Astrophys. J. **500**, 411 (1998)
31. Dent, W.R.F., Greaves, J.S., Coulson, I.M.: Mon. Not. R. Astron. Soc. **359**, 663 (2005)

32. Dullemond, C.P., Dominik, C., Natta, A.: Astrophys. J. **560**, 957 (2001)
33. Dullemond, C.P., Monnier, J.D.: Annu. Rev. Astron. Astrophys. **48**, 205 (2010)
34. Dullemond, C.P., van den Ancker, M.E., Acke, B., van Boekel, R.: Astrophys. J. Lett. **594**, L47 (2003)
35. Eisner, J.A., Lane, B.F., Hillenbrand, L.A., Akeson, R.L., Sargent, A.I.: Astrophys. J. **613**, 1049 (2004)
36. Espaillat, C., Muzerolle, J., Hernández, J., et al.: Astrophys. J. Lett. **689**, L145 (2008)
37. Folsom, C.P., Bagnulo, S., Wade, G.A., et al.: Mon. Not. R. Astron. Soc. **422**, 2072 (2012)
38. Furlan, E., Hartmann, L., Calvet, N., et al.: Astrophys. J. Suppl. Ser. **165**, 568 (2006)
39. Garrison, L.M. Jr.: Astrophys. J. **224**, 535 (1978)
40. Ghandour, L., Strom, S., Edwards, S., Hillenbrand, L.: In: The, P.S., Perez, M.R., van den Heuvel, E.P.J. (eds.) The Nature and Evolutionary Status of Herbig Ae/Be Stars. Astronomical Society of the Pacific Conference Series, vol. 62, p. 223 (1994)
41. Grady, C.A., Polomski, E.F., Henning, T., et al.: Astron. J. **122**, 3396 (2001)
42. Grady, C.A., Woodgate, B., Heap, S.R., et al.: Astrophys. J. **620**, 470 (2005)
43. Grasdalen, G.L., Strom, S.E., Strom, K.M., et al.: Astrophys. J. Lett. **283**, L57 (1984)
44. Grinin, V.P., Kozlova, O.V., Natta, A., et al.: Astron. Astrophys. **379**, 482 (2001)
45. Hartmann, L., Kenyon, S.J., Calvet, N.: Astrophys. J. **407**, 219 (1993)
46. Herbig, G.H.: Astrophys. J. Suppl. Ser. **4**, 337 (1960)
47. Herbst, W., Shevchenko, V.S.: Astron. J. **118**, 1043 (1999)
48. Hernández, J., Calvet, N., Briceño, C., et al.: Astrophys. J. **671**, 1784 (2007)
49. Hernández, J., Calvet, N., Hartmann, L., et al.: Astron. J. **129**, 856 (2005)
50. Hernández, J., Hartmann, L., Megeath, T., et al.: Astrophys. J. **662**, 1067 (2007)
51. Hillenbrand, L.A., Strom, S.E., Vrba, F.J., Keene, J.: Astrophys. J. **397**, 613 (1992)
52. Joy, A.H.: Astrophys. J. **102**, 168 (1945)
53. Kenyon, S.J., Hartmann, L.: Astrophys. J. **323**, 714 (1987)
54. Kim, K.H., Watson, D.M., Manoj, P., et al.: Astrophys. J. **700**, 1017 (2009)
55. Kraus, A.L., Ireland, M.J.: Astrophys. J. **745**, 5 (2012)
56. Lada, C.J., Adams, F.C.: Astrophys. J. **393**, 278 (1992)
57. Lagage, P.-O., Doucet, C., Pantin, E., et al.: Science **314**, 621 (2006)
58. Lommen, D.J.P., van Dishoeck, E.F., Wright, C.M., et al.: Astron. Astrophys. **515**, A77 (2010)
59. Lynden-Bell, D., Pringle, J.E.: Mon. Not. R. Astron. Soc. **168**, 603 (1974)
60. Mannings, V., Sargent, A.I.: Astrophys. J. **490**, 792 (1997)
61. Mannings, V., Sargent, A.I.: Astrophys. J. **529**, 391 (2000)
62. Meeus, G., Waters, L.B.F.M., Bouwman, J., et al.: Astron. Astrophys. **365**, 476 (2001)
63. Monnier, J.D., Millan-Gabet, R.: Astrophys. J. **579**, 694 (2002)
64. Mora, A., Eiroa, C., Natta, A., et al.: Astron. Astrophys. **419**, 225 (2004)
65. Mora, A., Natta, A., Eiroa, C., et al.: Astron. Astrophys. **393**, 259 (2002)
66. Natta, A., Kruegel, E.: Astron. Astrophys. **302**, 849 (1995)
67. Natta, A., Prusti, T., Neri, R., et al.: Astron. Astrophys. **371**, 186 (2001)
68. Okamoto, Y.K., Kataza, H., Honda, M., et al.: Astrophys. J. **706**, 665 (2009)
69. Pantin, E., Waelkens, C., Lagage, P.O.: Astron. Astrophys. **361**, L9 (2000)
70. Pinte, C., Padgett, D.L., Ménard, F., et al.: Astron. Astrophys. **489**, 633 (2008)
71. Pontoppidan, K.M., Salyk, C., Blake, G.A., et al.: Astrophys. J. **720**, 887 (2010)
72. Rodgers, B., Wooden, D.H., Grinin, V., Shakhovsky, D., Natta, A.: Astrophys. J. **564**, 405 (2002)
73. Stapelfeldt, K.R., Krist, J.E., Menard, F., et al.: Astrophys. J. Lett. **502**, L65 (1998)
74. Strom, K.M., Strom, S.E., Edwards, S., Cabrit, S., Skrutskie, M.F.: Astron. J. **97**, 1451 (1989)
75. Suzuki, T.K., Inutsuka, S.-I.: Astrophys. J. Lett. **691**, L49 (2009)
76. Testa, P., Huenemoerder, D.P., Schulz, N.S., Ishibashi, K.: Astrophys. J. **687**, 579 (2008)
77. The, P.S., de Winter, D., Perez, M.R.: Astron. Astrophys. Suppl. Ser. **104**, 315 (1994)
78. Uchida, K.I., Calvet, N., Hartmann, L., et al.: Astrophys. J. Suppl. Ser. **154**, 439 (2004)
79. van den Ancker, M.E., The, P.S., de Winter, D.: Astron. Astrophys. **309**, 809 (1996)
80. van Dishoeck, E.F.: Annu. Rev. Astron. Astrophys. **42**, 119 (2004)

81. Varnière, P., Blackman, E.G., Frank, A., Quillen, A.C.: Astrophys. J. **640**, 1110 (2006)
82. Waters, L.B.F.M., Waelkens, C.: Annu. Rev. Astron. Astrophys. **36**, 233 (1998)
83. Weidenschilling, S.J.: Icarus **127**, 290 (1997)
84. Williams, J.P., Cieza, L.A.: Annu. Rev. Astron. Astrophys. **49**, 67 (2011)
85. Wyatt, M.C.: Annu. Rev. Astron. Astrophys. **46**, 339 (2008)
86. Zinnecker, H., Yorke, H.W.: Annu. Rev. Astron. Astrophys. **45**, 481 (2007)